

# Study of time-like electromagnetic form factors of $\Lambda$ , $\Sigma$ and $\Xi^+$ in light-front quark model

Chong-Chung Lih<sup>a</sup> and Chao-Qiang Geng<sup>b</sup>

*Chongqing University of Posts and Telecommunications, Chongqing, 400065, China*

*School of Fundamental Physics and Mathematical Sciences,*

*Hangzhou Institute for Advanced Study, UCAS, Hangzhou 310024, China*

(Dated: January 6, 2026)

## Abstract

We use the light front quark model to investigate the form factors in the  $e^+e^- \rightarrow B\bar{B}$  collision processes with  $B = \Lambda$ ,  $\Sigma$  and  $\Xi$ . These form factor behaviors are calculated based on the Bethe-Salpeter formalism with  $q^+ > 0$  to effectively account for non-valence contributions. We show that our results of the  $q^2$ -dependent form factors closely match the BESIII data. In particular, we obtain that  $|G_{eff}| = (0.921, 0.098, 0.189)$  and  $R = |\frac{G_E}{G_M}| = (0.97, 0.89, 0.936)$  for  $e^+e^- \rightarrow \Lambda\bar{\Lambda}$ ,  $\Sigma^+\Sigma^-$ ,  $\Xi^+\Xi^+$ ) which  $q^2 = (5.74, 6.0, 7.0)$  GeV $^2$ .

---

<sup>a</sup> ccli123@gmail.com

<sup>b</sup> cqgeng@ucas.ac.cn

## I. INTRODUCTION

Understanding the internal structure of hadrons has always been a great challenge. Quantum chromodynamics (QCD) uses quarks and gluons (i.e., QCD degrees of freedom) to describe the structure of hadrons and their interactions. We are accustomed to believe that the motion of quarks and gluons inside hadrons will change under the action of strong fields in nuclear matter, and such changes are expected to be reflected in the electromagnetic and weak structures of nucleons and other baryons [1–3]. A commonly used parameter for the electromagnetic structure of hadrons is the electromagnetic form factor (EMFF), which is an observable quantity of non-perturbative QCD and is also a key to understand bound-state QCD effects. Therefore, the EMFF can be used to explore the internal structure of baryons and experimentally detected through the interaction of hadrons with virtual photons.

Another possibility for revealing the electromagnetic structure of baryons is the  $e^+e^-$  scattering. It allows us to enter the time-like regime ( $q^2 = -Q^2 \geq 0$ ), which was proposed long ago by Cabibbo and Gatto [5]. The  $e^+e^- \rightarrow B\bar{B}$  (and its inverse) reaction offers new opportunities for studying valence quark effects, diquark pairs (diquarks), and the role of different quark compositions [6–12]. This time-like form factor appears to be a viable tool for determining hyperon structures, both near the threshold and in the larger  $q^2$  region, where perturbation effects are expected to be dominated [4, 5, 11–16]. In recent years, experiments with  $e^+e^- \rightarrow B\bar{B}$  and  $p^+p^- \rightarrow B\bar{B}$  experiments [20–25] have been able to detect the structure of short-lived baryons in the timelike kinematic region above the threshold  $4M_B^2$  (where  $M_B$  is the baryon mass). The experiments at BaBar [17], BESIII [18, 19] and CLEO [11, 12] have also provided data related to the electromagnetic form factor of timelike hyperons. These timelike studies complement our understanding of the spacelike region ( $q^2 \leq 0$ ) [26–28] based on electron scattering experiments over the past two decades.

The light front quark model (LFQM), a phenomenological model previously used extensively to study the form factors of meson weak decays, operates not only directly in the time-like regime but also in the space-like regime. Using the “+” component of the current in the Drell-Yan-West ( $q^+ = q_0 + q_z = 0$ ) framework, the form factors of decays in the space-like regime ( $q^2 < 0$ ) can be calculated, along with contributions from valence and Folk states. Another option is to use the same “+” component but in the  $q^+ \neq 0$  regime, i.e., the timelike regime ( $q^2 > 0$ ). Physically, particle decay processes occur in the time-like regime, so in

principle, the form factors can be calculated in the  $q^+ \neq 0$  framework in the time-like regime. However, operating in the time-like regime may yield contributions from non-valence Fock states [29], requiring the wave function to have higher Fock states. This means that we will inevitably encounter nonvalence diagrams arising from the production of quark-antiquark pairs. As shown in Figures 1(b) and (c), the collision process  $e^+e^- \rightarrow B\bar{B}$  is a typical non-valence diagram. Fortunately, the literature already provides effective methods for dealing with non-valence contributions in meson-incompatible processes [29–32]. The goal of our method is to use this procedure to directly calculate the form factor in the  $e^+e^- \rightarrow B\bar{B}$  collision process and compare it with the experimental data.

This paper is organized as follows. In Sec. II, we present the framework for the form factors of  $e^+e^- \rightarrow B\bar{B}$ . Our numerical results and discussions are given in Sec. III. We conclude in Sec. IV.

## II. A FRAMEWORK FOR $e^+e^- \rightarrow B\bar{B}$

The reaction where a lepton pair  $l^+l^-$  into a  $B\bar{B}$  pair, viz

$$l^+l^- \rightarrow \gamma^* \rightarrow B\bar{B}, \quad (1)$$

is a direct source of information on nuclear form factors in the time-like region. These is a one-photon-exchange for the electron–positron annihilation into a  $B\bar{B}$  pair and is produced only for  $q^2 \geq 4M_B^2$ . In particular, to investigate the process of Eq. (1), the matrix elements of the nucleon current operator involved in this reaction are written as follows,

$$\sqrt{\frac{EE'}{M_B^2}}(2\pi)^3 \langle \mathcal{B}(p, s)\mathcal{B}'(p', s') | J_{em}^\mu(0) | 0 \rangle = \bar{u}_s(P) \left[ \gamma^\mu f_1(q^2) + i \frac{f_2(q^2)}{2M_B} \sigma^{\mu\nu} q_\nu \right] v_{S'}(P'), \quad (2)$$

where  $q^\mu = P^\mu + P'^\mu$  and  $f_i(i = 1, 2)$  are the baryonic form factors. In the time-like region, the current operator participates in transitions from vacuum to a state containing hadron pairs, which becomes a real state beyond the intrinsic threshold given by  $q^2 = 4M_B^2$ .

Employing the single-photon approximation, the form shown in Eq. (2) is the most general possible form, but it is not the only concise expression. For the baryon pair production differential cross section, after transforming from the center-of-mass frame to the laboratory frame, we obtain: [5, 33, 34],

$$\frac{d\sigma}{d\Omega} |_{(l^+l^- \rightarrow B\bar{B})} = \frac{\alpha^2 \beta}{4q^2} \left\{ (1 + \cos^2 \theta) |G_M(q^2)|^2 + \frac{\sin^2 \theta}{\tau} |G_E(q^2)|^2 \right\}, \quad (3)$$

where  $\alpha$  is fine structure constant,  $\beta = \sqrt{1 - \frac{4M_B^2}{q^2}}$ ,  $\tau = \frac{q^2}{4M_B^2}$ ,  $\theta$  is the angle between the direction of the incoming electron and the produced hardron,  $G_E(q^2)$  and  $G_M(q^2)$  are the charge and magnetic form factor, respectivly. In comparison to Eq. (2), one has

$$G_E = f_1(q^2) + \tau f_2(q^2), \quad G_M = f_1(q^2) + f_2(q^2). \quad (4)$$

Compared to the traditional form factors  $f_1(q^2)$  and  $f_2(q^2)$ , the simplified charge form factor  $G_E(q^2)$  and magnetic form factor  $G_M(q^2)$  provide greater clarity for discussing experimental data. Integrating the solid angle  $\Omega$  over the expression Eq. (3), one obtains

$$\sigma_{(l+l \rightarrow B\bar{B})} = \frac{4\pi\alpha^2\beta}{3q^2} \left\{ |G_M(q^2)|^2 + \frac{|G_E(q^2)|^2}{2\tau} \right\} \quad (5)$$

According to Eq. (2), to calculate the form factors, we employe a light-front quark model in the time-like region. In the LFQM, we treat baryons containing three quarks as bound states composed of a single quark  $q_1$  and a diquark  $q_{[2,3]}$ , wherein the diquark  $q_{[2,3]}$  comprises  $q_2$  and  $q_3$ . Explicitly, the baryon bound state with the total momentum  $P$  and spin  $S = \frac{1}{2}$  can be written as [48]

$$|\mathcal{B}(P, S, S_z)\rangle = \int \{d^3p_1\} \{d^3p_{[q_2, q_3]}\} 2(2\pi)^3 \delta^3(\tilde{P} - \tilde{p}_1 - \tilde{p}_{[q_2, q_3]}) \times \sum_{\lambda_1, \lambda_2} \Psi^{SS_z}(\tilde{p}_1, \tilde{p}_{[q_2, q_3]}, \lambda_1, \lambda_2) |q_1(p_1, \lambda_1) [q_2, q_3](p_{[q_2, q_3]}, \lambda_2)\rangle, \quad (6)$$

where  $q_1$  denotes the active quark of the baryon,  $[q_2, q_3]$  represents the diquark,  $\Psi^{SS_z}$  corresponds to the momentum-space wave function and  $p_{1,2}$  are the on-mass-shell light front momenta,

$$\tilde{p} = (p^+, p_\perp), \quad p_\perp = (p^1, p^2), \quad p^- = \frac{m^2 + p_\perp^2}{p^+}, \quad (7)$$

with

$$p_1^+ = x_1 P^+, \quad p_{[q_2, q_3]}^+ = x_2 P^+, \quad x_1 + x_2 = 1, \\ p_{1\perp} = x_1 P_\perp + k_\perp, \quad p_{[q_2, q_3]\perp} = x_2 P_\perp - k_\perp. \quad (8)$$

In Eq. (8),  $(x, k_\perp)$  are the light-front relative momentum variables, and  $\vec{k}_\perp$  is the component of the internal momentum  $\vec{k} = (\vec{k}_\perp, k_z)$ .

By the Melosh transformation [36], it is more convenient to work with the following representation of the wave function

$$\Psi^{SS_z}(\tilde{p}_1, \tilde{p}_{[q_2, q_3]}, \lambda_1, \lambda_2) = \frac{1}{\sqrt{2(p_1 \cdot \bar{P} + m_1 M_0)}} \bar{u}(p_1, \lambda_1) \Gamma_{l,m} u(\bar{P}, S_z) \phi(x, k_\perp), \quad (9)$$

where  $\Gamma_{l,m}$  is the coupling vertex function of the decaying quark  $q_1$  and the diquark in the baryon state. For the scalar diquark, the coupling vertex is  $\Gamma_s = 1$ . If the axial-vector diquark is involved, the vertex should be

$$\Gamma_A = -\frac{1}{\sqrt{3}}\gamma_5 \not{e}^*(p_{[q_2,q_3]}, \lambda_2). \quad (10)$$

The wave function of  $\phi(x, k_\perp)$  in Eq. (9) describes the momentum distribution of the constituent quarks in the bound state. In this work, we use the Gaussian-type function, given as

$$\phi(x, k_\perp) = 4 \left( \frac{\pi}{\beta^2} \right)^{3/4} \sqrt{\frac{dk_z}{dx}} \exp \left( \frac{-\vec{k}^2}{2\beta^2} \right), \quad (11)$$

where  $\beta$  is the baryon sharp parameter and  $k_z$  is defined by

$$k_z = \frac{xM_0}{2} - \frac{m_2^2 + k_\perp^2}{2xM_0}, \quad M_0 = e_1 + e_2, \quad (12)$$

and

$$M_0^2 = \frac{m_1^2 + k_\perp^2}{1-x} + \frac{m_2^2 + k_\perp^2}{x}. \quad (13)$$

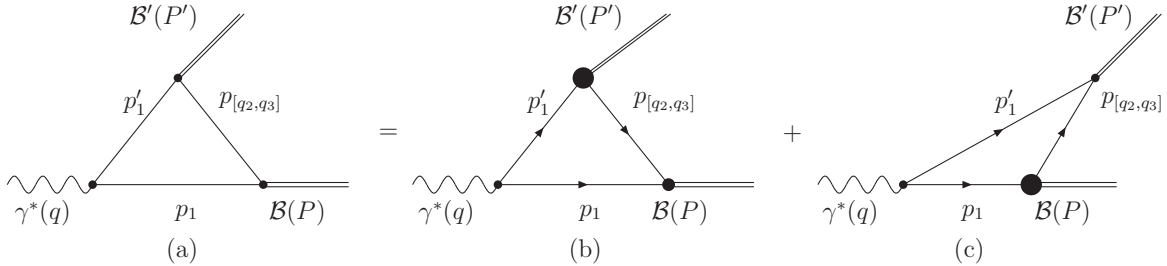


FIG. 1. The effective treatment of the LF amplitude (a) can be displayed into two parts in the regions of (b)  $0 < x < \alpha$  and (c) in  $\alpha < x < 1$ , where the small and big dots of the mediator-quark vertices in (b) and (c) represent the LF ordinary and nonvalence wavefunction vertices, respectively.

In our calculation, we assume

$$\alpha \equiv \frac{P^+}{q^+} = \frac{q^2 + M_B^2 - M_{B'}^2 - \sqrt{(q^2 + M_B^2 - M_{B'}^2) - 4M_B^2 q^2}}{2q^2}. \quad (14)$$

Using the bound states of  $|\mathcal{B}(P, S, S_z)\rangle$  and  $|\mathcal{B}'(P', S', S'_z)\rangle$  in Eq. (6) and the above identities, we derive the matrix elements of the baryonic transition in the LF frame. By considering

the  $\mu = +$  component, the transition matrix elements are given by

$$\begin{aligned} & \langle \mathcal{B}(P, S, S_z) \mathcal{B}'(P', S', S'_z) | \bar{q} \gamma^\mu Q | 0 \rangle \\ &= N_{fs} \int \{d^3 p_2\} \frac{\Psi(x, \mathbf{k}_\perp) I^+ \Psi'(x', \mathbf{k}'_\perp)}{(1-x)(1-x')} , \end{aligned} \quad (15)$$

where  $I^+ = \sum_{\lambda_2} \bar{u}(\bar{P}', S'_z) \left[ \bar{\Gamma}'_{S(A)}(p''_1 + m'_1) \gamma^+(p'_1 + m_1) \Gamma_{S(A)} \right] u(\bar{P}, S_z)$ ,  $\bar{\Gamma} = \gamma^0 \Gamma^\dagger \gamma^0$  and  $N_{fs}$  is a flavor-spin factor to be given for different processes. The trace term  $I^+$  in Eq. (15) can be written as the sum of  $I_1^+$  and  $I_2^+$ , as shown in Fig. 1. In the region of  $0 < x < \alpha$  with  $0 < p_1^+ < P'^+$  and  $p_1^- = p_{1on}^- = (m_1^2 + k_\perp^2)/p_1^+$ , the baryon  $\mathcal{B}'$  will possess a nonvalence vertex, as seen in Fig. 1(b). The effective contribution of the LF amplitude is given by [37–40]

$$\begin{aligned} \mathcal{M} &= \frac{N_{fs}}{16\pi^3} \int_0^\alpha dx \int d^2 \mathbf{k}_\perp \frac{\Psi(x, \mathbf{k}_\perp) I_V^+ \Psi'(x', \mathbf{k}_\perp)}{(1-x)(1-x')} , \\ I_1^+ &= \bar{u}(\bar{P}', S'_z) \bar{\Gamma}'(p''_1 + m'_1) \gamma^+(p'_1 + m_1) \Gamma u(\bar{P}, S_z) . \end{aligned} \quad (16)$$

The wave function corresponding to the nonvalence vertex is usually obtainable from the Bethe-Salpeter (BS) amplitude in the BS theory [41, 42]. The LF BS equation is expressed as [42–44]

$$(M^2 - M_0^2) \Psi_B(x_i, k_{i\perp}) = \int [dy] [d^2 \mathbf{l}_\perp] \mathcal{K}(x, \mathbf{k}_\perp; y, \mathbf{l}_\perp) \Psi_B(y, \mathbf{l}_\perp) . \quad (17)$$

The nonvalence BS amplitudes can be regarded as solutions of Eq. (17). For the baryon  $\mathcal{B}$ , the normal and nonvalence BS amplitudes correspond to  $x > \alpha$  and  $x < \alpha$ , respectively. In Fig. 1(b), the nonvalence B-S amplitude is the analytic continuation of the valence BS amplitude. In the LFQM, the relationship between the BS amplitudes of two regions is given in Refs. [42, 45, 46]. However, for the integral equation of Eq. (17) it is necessary to use the nonperturbative QCD method to obtain the kernel. Following Refs. [37–40], we obtain the transition form factors:

$$\begin{aligned} f_1(q^2) &= \frac{N_{fs}}{16\pi^3} \int_\alpha^1 dx \int d^2 \mathbf{k}_\perp \frac{\Gamma_g(x, \mathbf{k}_\perp) I_{f_1}^+}{(1-x)(x'-1)P^+P'^+} \Psi_{\mathcal{B}}(x, \mathbf{k}_\perp) \\ &\quad \times \int \frac{dy}{y(1-y)} \int d^2 \mathbf{l}_\perp \mathcal{K}(x, \mathbf{k}_\perp; y, \mathbf{l}_\perp) \Psi_{\mathcal{B}'}(y, \mathbf{l}_\perp) , \\ I_{f_1}^+ &= \text{Tr}[(\not{p}' + M') \gamma^+ (\not{p} + M) (\not{p}'_1 + m'_1) \gamma^+ (\not{p}_1 + m_1)] , \\ \frac{f_2(q^2)}{M_{\mathcal{B}} + M_{\mathcal{B}'}} &= \frac{N_{fs}}{16\pi^3} \int_\alpha^1 dx \int d^2 \mathbf{k}_\perp \frac{\Gamma_g(x, \mathbf{k}_\perp) I_{f_2}^+}{(1-x)(x'-1)P^+P'^+ q_\perp^\nu} \Psi_{\mathcal{B}}(x, \mathbf{k}_\perp) \\ &\quad \times \int \frac{dy}{y(1-y)} \int d^2 \mathbf{l}_\perp \mathcal{K}(x, \mathbf{k}_\perp; y, \mathbf{l}_\perp) \Psi_{\mathcal{B}'}(y, \mathbf{l}_\perp) , \\ I_{f_2}^+ &= \text{Tr}[(\not{p}' + M') \sigma^{\nu+} (\not{p} + M) (\not{p}'_1 + m'_1) \gamma^+ (\not{p}_1 + m_1)] . \end{aligned} \quad (18)$$

where  $\nu = 1, 2$  and the trace term in Eq. (18) should be separated into the on-shell propagating and instantaneous parts of  $I_{on}^\mu$  and  $I_{inst}^\mu$  via

$$\not{p} + m = (\not{p}_{on} + m) + \frac{1}{2}\gamma^+(p^- - p_{on}^-), \quad (19)$$

respectively. The explicit forms of the above form factors can be expressed as functions of the internal variables of  $x$  and  $k_\perp$ . In Eq. (18),  $\Gamma_g$  is a vertex function for the gauge boson associated with the LF energy denominator with its explicit form given by [42, 46, 47]

$$\Gamma_g^{-1}(x, \mathbf{k}_\perp) = \alpha \left[ \frac{q^2}{1-\alpha} - \left( \frac{\mathbf{k}_\perp^2 + m_1^2}{1-x} + \frac{\mathbf{k}'_\perp^2 + m'_1^2}{x-\alpha} \right) \right]. \quad (20)$$

The trace terms in Eqs. (16) and (18), both corresponding to the products of the initial and final LF spin wave functions, can be obtained by off-shell Meloche transformations. The form factors related to Fig. 1(b) are given by

$$\begin{aligned} f_{1_{NV}}(q^2) &= \frac{N_{fs}}{16\pi^3} \int_\alpha^1 dx \int d^2\mathbf{k}_\perp \Gamma_g(x, \mathbf{k}_\perp) \Psi_i(x, \mathbf{k}_\perp) \\ &\times \frac{[k_\perp \cdot k'_\perp + ((1-x_1)M_0 + m_1)((1-x'_1)M' + m'_1)] + I_{inst}^+}{(1-x)(x'-1)} \\ &\times \int \frac{dy}{y(1-y)} \int d^2\mathbf{l}_\perp \mathcal{K}(x, \mathbf{k}_\perp; y, \mathbf{l}_\perp) \Psi_f(y, \mathbf{l}_\perp), \\ \frac{f_{2_{NV}}(q^2)}{M_B + M_{B'}} &= \frac{N_{fs}}{16\pi^3} \int_\alpha^1 dx \int d^2\mathbf{k}_\perp \Gamma_g(x, \mathbf{k}_\perp) \Psi_i(x, \mathbf{k}_\perp) \\ &\times \frac{[(m_1 + (1-x_1)M_0)k'_\perp \cdot q_\perp - (m'_1 + (1-x'_1)M')k_\perp \cdot q_\perp] + I_{inst}^{\prime+}}{(1-x)(x'-1)q_\perp^2} \\ &\times \int \frac{dy}{y(1-y)} \int d^2\mathbf{l}_\perp \mathcal{K}(x, \mathbf{k}_\perp; y, \mathbf{l}_\perp) \Psi_f(y, \mathbf{l}_\perp), \end{aligned} \quad (21)$$

In Eq. (19), the subscript “on” denotes the on-mass-shell and the instantaneous parts of the non-valence diagram associated with  $8p_{1on}^+ p_{1on}'^+ (M^2 - M_0^2) (\frac{m'_1}{1-x'} + M')$  in  $I_{NV}^+$ . It is worth noting that the instantaneous contribution exists in the non-valence diagram only when the “+” component is used.

The relevant operator  $\mathcal{K}$  in Eqs. (17), (18) and (21) is the BS core, which in principle contains contributions from high Fock states. It is the high Fock component of the bound state related to the lowest Fock component with this kernel. The kernel functions can be obtained by using the non-perturbative QCD. The kernel  $\mathcal{K}$  is a function of all internal

momenta  $(x, \mathbf{k}_\perp, y, \mathbf{l}_\perp)$ . We define that  $G_{\mathcal{B}_i \mathcal{B}_f} \equiv \int [dy] [d^2 \mathbf{l}_\perp] \mathcal{K}(x, \mathbf{k}_\perp; y, \mathbf{l}_\perp) \Psi_f(y, \mathbf{l}_\perp)$ , which depends only on  $x$  and  $\mathbf{k}_\perp$ . The range of the momentum fraction  $x$  relies on the external momenta for the embedded states.

In the region of  $\alpha < x < 1$ ,  $P'^+ < p^+ < P^+$  and  $p_1'^- = p_{1on}^-' = (m_1'^2 + k_{1\perp}^{'2})/p_1'^+$ . At this point, the vertex of the baryon  $\mathcal{B}$  enters the non-valence region, while the vertex of baryon  $\mathcal{B}'$  the valence region, as shown in Fig. 1(c). For the transition form factors, we may directly exchange the following parameters in Eq. (18):

$$x \leftrightarrow x', \quad m_1 \leftrightarrow m_1', \quad p_1 \leftrightarrow p_1', \quad \Psi_{\mathcal{B}} \leftrightarrow \Psi_{\mathcal{B}'} \quad (22)$$

### III. NUMERICAL RESULTS AND DISCUSSIONS

We present numerical results on the form factors of the  $e^+e^- \rightarrow B\bar{B}$  transitions in the time-like region for the LFQM. Computationally, we hope to find a time-domain-like result, so we only introduce  $q_\perp = 0$  in the final numerical calculation. In our calculations, we use [48]

$$m_{u,d} = 0.25, \quad m_s = 0.38, \quad m_{[qq]} = 0.7, \quad \beta_{s[qq]} = 0.4 \pm 0.05, \quad \beta_{u[qq]} = 0.2 \pm 0.1. \quad (23)$$

In Eq. (21),  $G_{\mathcal{B}_i \mathcal{B}_f}$  can be taken as a constant in the range of  $0.1 \sim 6.0$ , which was previously tested in some exclusively semileptonic decay processes and shown to be a good approximation for processes with a small momentum transfer [42, 46]. Explicitly, we choose  $G_{\mathcal{B}_i \mathcal{B}_f} = 1.8, 1.0$  and  $0.3$  for  $\Lambda\Lambda$ ,  $\Sigma^+\Sigma^+$  and  $\Xi^+\Xi^+$ , respectively, in our numerical evaluation.

To describe the momentum  $q^2$  behaviors, we parameterize the form factors in the double-pole forms of

$$F(q^2) = \frac{F(0)}{1 + a(q^2/m_P^2) + b(q^4/m_P^4)}, \quad (24)$$

with  $m_P = 6.0$  GeV for all modes of  $e^+e^- \rightarrow B\bar{B}$  in  $M_B$  mass scalar, and  $(F(0), a, b)$  to be determined in the numerical analysis. Our results for the form factors are given in Table I. In our results, the errors come from uncertainties in the parameters of  $\beta$ .

In Fig. 2, we present our evaluations of the form factors as functions of  $q^2$  for the  $e^+e^- \rightarrow \Lambda\Lambda$ ,  $\Sigma^+\Sigma^-$  and  $\Xi^+\Xi^-$  transitions, respectively, where the BESIII data fits are also given. From the figures, we compare the LF model calculations for  $|G_{eff}|$  with the BESIII data of  $\Lambda\Lambda$ ,  $\Sigma^+\Sigma^-$ , and  $\Xi^+\Xi^-$  for  $q^2 \geq 10$  GeV $^2$ . This comparison shows that the LF model describes

TABLE I. From factors of the  $e^+e^- \rightarrow B\bar{B}$  transition

$e^+e^- \rightarrow \Lambda\Lambda$	$F(q^2 = 5.7408 \text{ GeV}^2)$	$a$	$b$
$G_E$	$0.456^{+0.112}_{-0.074}$	-193.38	1391.17
$G_M$	$0.462^{+0.113}_{-0.078}$	-157.969	1133.79
$e^+e^- \rightarrow \Sigma^+\Sigma^-$	$F(q^2 = 6.0 \text{ GeV}^2)$	$a$	$b$
$G_E$	$0.0451^{+0.0041}_{-0.0003}$	-14.716	91.45
$G_M$	$0.0512^{+0.0036}_{-0.0002}$	-13.478	83.93
$e^+e^- \rightarrow \Xi^+\Xi^-$	$F(q^2 = 7.0 \text{ GeV}^2)$	$a$	$b$
$G_E$	$0.0903^{+0.0237}_{-0.0156}$	-74.80	384.711
$G_M$	$0.0965^{+0.0245}_{-0.0164}$	-53.141	273.371

the data well above  $q^2 \geq 10 \text{ GeV}^2$  within the theoretical limit. Current calculations for  $|G_{eff}|$  indicate that the region  $q^2 \geq 10 \text{ GeV}^2$  is within the range, where the asymptotic behavior of the form factor can be observed. However, it is important to note that the current data may still be in the non-perturbative QCD regime.

Fig. 2 shows that the four form factors exhibit a similar behaviors throughout the  $q^2$  spectra. Obviously, our LFQM results with the non-valence contributions are consistent with the BESIII data [49–51]. We also use this model to calculate the  $|G_E/G_M|$  ratios for the processes  $e^+e^- \rightarrow (\Lambda\bar{\Lambda}, \Sigma^+\Sigma^-, \Xi^+\Xi^-)$ . For the three processes mentioned above, at  $q^2 = (5.7408, 6.0, 7.0) \text{ GeV}^2$ , we get  $|G_{eff}| = (0.921^{+0.22}_{-0.15}, 0.098^{+0.002}_{-0.0002}, 0.189^{+0.048}_{-0.032})$  and  $R = |\frac{G_E}{G_M}| = (0.985 \pm 0.001, 0.88 \pm 0.01, 0.936 \pm 0.004)$ .

#### IV. CONCLUSION

The  $e^+e^-$  collision experiments explore the electromagnetic properties of elementary particles. Under the electromagnetic interaction at the tree level,  $e^+e^-$  annihilation processes can occur via virtual photons with timelike four-moments, which subsequently decay into final states. In this work, we have used the LFQM to investigate the form factors in the  $e^+e^- \rightarrow B\bar{B}$  collision processes. In particular, we have analyzed the form factors for the baryon transition based on the BS formalism with  $q^+ > 0$ , effectively accounting for nonvalence contributions. We have found that the  $q^2$  behaviors of the form fac-

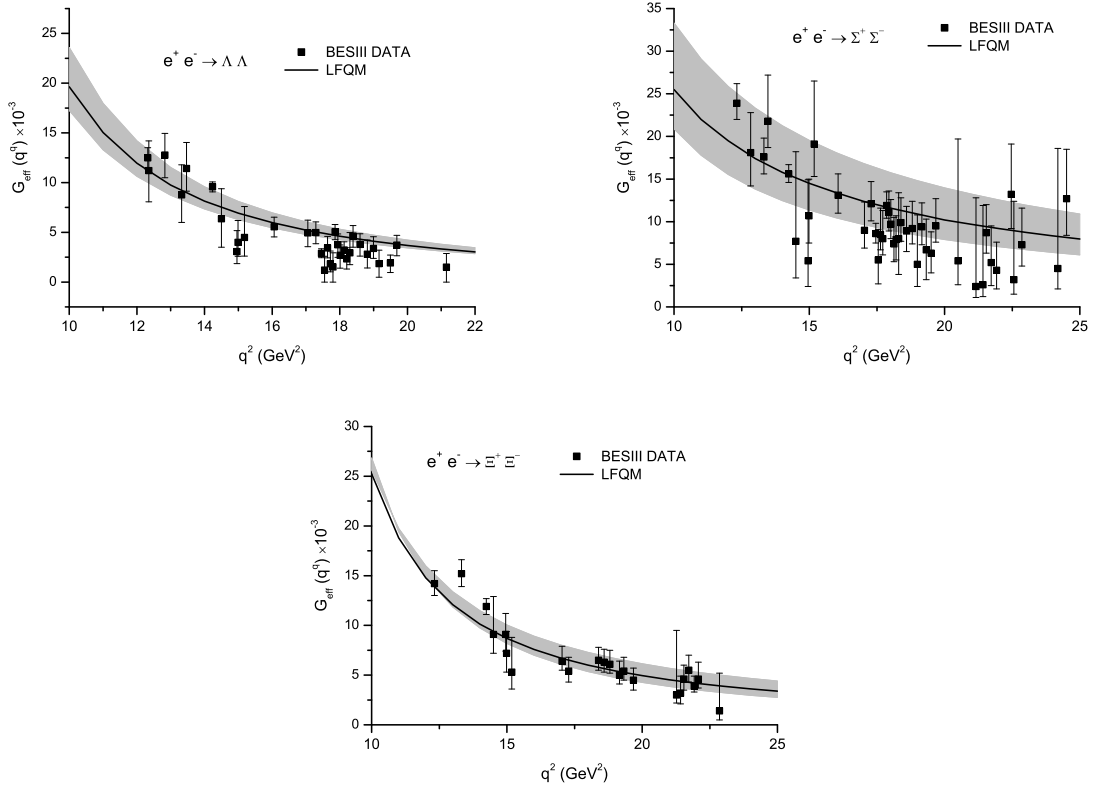


FIG. 2. Form factors of  $e^+e^- \rightarrow B\bar{B}$ .

tors are consistent with the experimental data at BESIII. As shown in Table 2, for the processes of  $e^+e^- \rightarrow (\Lambda\bar{\Lambda}, \Sigma^+\Sigma^-, \Xi^+\Xi^-)$  at  $q^2=(5.74, 6.0, 7.0)$   $\text{GeV}^2$ , our results are  $|G_{eff}| = (0.921, 0.098, 0.189)$  and  $R = |G_E/G_M| = (0.97, 0.89, 0.936)$ , respectively. These results with nonvalence contributions agree with the existing BESIII experimental data and other theoretical estimates.

## ACKNOWLEDGMENTS

This work is supported in part by the National Natural Science Foundation of China (NSFC) under Grant No. 12547104.

[1] G. E. Brown, M. Rho, Phys. Rev. Lett. (1991), 66, 2720.

[2] W. K. Brooks, S. Strauch and K. Tsushima, J. Phys. Conf. Ser. (2011), 299, 012011.

- [3] K. Saito, K. Tsushima and A. W. Thomas, *Prog. Part. Nucl. Phys.* (2007), 58, 1.
- [4] S. Pacetti, R. Baldini Ferroli and E. Tomasi-Gustafsson, *Phys. Rept.* 550-551, 1 (2015).
- [5] N. Cabibbo and R. Gatto, *Phys. Rev.* 124, 1577(1961).
- [6] P. Kroll, T. Pilsner, M. Schurmann and W. Schweiger, *Phys. Lett.* B316, 546(1993).
- [7] R. Jakob, P. Kroll, M. Schurmann and W. Schweiger, *Z. Phys.* A347, 109(1993).
- [8] R. L. Jaffe and F. Wilczek, *Phys. Rev. Lett.* 91, 232003 (2003).
- [9] F. Wilczek, in *From fields to strings*, edited by M. Shifman, Vol.1, pp77-93(2005).
- [10] A. Selem and F. Wilczek, *New Trends HERA Phys.* 2005, 337(2006).
- [11] S. Dobbs, K. K. Seth, A. Tomaradze, T. Xiao and G. Bonvicini, *Phys. Rev. D* 96, 092004 (2017) [arXiv:1708.09377 [hep-ex]].
- [12] S. Dobbs, A. Tomaradze, T. Xiao, K. K. Seth and G. Bonvicini, *Phys. Lett. B* 739, 90 (2014) [arXiv:1410.8356 [hep-ex]]. 14
- [13] B. Aubert et al. [BaBar Collaboration], *Phys. Rev. D* 73, 012005 (2006).
- [14] K. K. Seth, S. Dobbs, Z. Metreveli, A. Tomaradze, T. Xiao and G. Bonvicini, *Phys. Rev. Lett.* 110, 022002 (2013).
- [15] K. Schonning and C. Li, *EPJ Web Conf.* 137, 12002 (2017).
- [16] C. Li [BESIII Collaboration], *J. Phys. Conf. Ser.* 742, 012020 (2016).
- [17] B. Aubert et al. [BaBar Collaboration], *Phys. Rev. D* 76, 092006 (2007).
- [18] M. Ablikim et al. [BESIII Collaboration], *Phys. Rev. D* 87, 11, 112011 (2013).
- [19] M. Ablikim et al. [BESIII Collaboration], *Phys. Rev. D* 97, 032013 (2018).
- [20] M. Ablikim et al. [BESIII], *Phys. Rev. D* 91 (2015) 112004.
- [21] M. Ablikim et al. [BESIII], *Chin. Phys. C* 44 (2020) 040001.
- [22] S. Dobbs, K. K. Seth, A. Tomaradze, T. Xiao and G. Bonvicini, *Phys. Rev. D* 96 (2017) 092004.
- [23] M. Ablikim et al. [BESIII], *Phys. Rev. Lett.* 123, (2019) 122003.
- [24] Ablikim et al. [BESIII], *Phys. Rev. Lett.* 132 (2024) 081904.
- [25] G. Ramalho, M. T. Pena and K. Tsushima, *Phys. Rev. D* 101 (2020) 014014.
- [26] I. G. Aznauryan, A. Bashir, V. Braun, S. J. Brodsky, V. D. Burkert, L. Chang, C. Chen, B. El-Bennich, I. C. Cloet and P. L. Cole, et al. *Int. J. Mod. Phys. E* 22 (2013) 1330015.
- [27] I. G. Aznauryan and V. D. Burkert, *Prog. Part. Nucl. Phys.* 67 (2012) 1.
- [28] G. Ramalho and M. T. Pena, *Prog. Part. Nucl. Phys.* 136 (2024) 104097.

[29] S. J. Brodsky and D. S. Hwang, Nucl. Phys. B 543, 239 (1998); C. R. Ji and H. M. Choi, Phys. Lett. B 513, 330 (2001).

[30] C. R. Ji and H. M. Choi, eConf C010430:T23 (2001).

[31] H. M. Choi, C. R. Ji, and L. S. Kisslinger, Phys. Rev. D 64, 093006 (2001).

[32] Chong-Chung Lih and Chao-Qiang Geng, Phys. Rev. D 112, 076023 (2025).

[33] Achim Denig and Giovanni Salme, Prog. Part. Nucl. Phys. 68 (2013) 113.

[34] A. Zichichi, S.M. Berman, N. Cabibbo, R. Gatto, IL Nuovo Cimento XXIV (1962) 170.

[35] H. G. Dosch, M. Jamin and B. Stech, Z. Phys. C **42**, 167 (1989).

[36] H. J. Melosh, Phys. Rev. **D 9**, 1095 (1974).

[37] Salam Tawfiq, Patrick J. O'Donnell and J.G. Korner, Phys. Rev. **D 58** 054010 (1998).

[38] Hans-Christian Pauli, Nucl. Phys. Proc. Suppl. **90** (2000) 259-272

[39] G. P. Lepage and S.J. Brodsky, Phys. Rev. **D 22**, 2157 (1980).

[40] Felix Schlumpf, Phys. Rev. D 47 (1993) 4114; Phys. Rev. **D 49** (1994) 6246 (erratum).

[41] B. L. G. Bakker and C. -R. Ji, Phys. Rev. **D 62**, 074014 (2000); B. L. G. Bakker, H. -M. Choi, and C. -R. Ji, Phys. Rev. **D 63**, 074014 (2001).

[42] S. J. Brodsky and D. S. Hwang, Nucl. Phys. **B 543**, 239 (1998); C. R. Ji and H. M. Choi, Phys. Lett. **B 513**, 330 (2001).

[43] S. J. Brodsky, C.-R. Ji and M. Sawicki, Phys. Rev. **D 32**, 1530 (1985).

[44] J. H. O. Sales, T. Frederico, B. V. Carlson, and P. U. Sauer, Phys. Rev. **C 61**, 044003 (2000).

[45] C. R. Ji and H. -M. Choi, eConf C010430:T23 (2001).

[46] H. M. Choi, C. R. Ji, and L. S. Kisslinger, Phys. Rev. **D 64**, 093006 (2001)

[47] H. M. Choi, C. R. Ji and L. S. Kisslinger, Phys. Rev. **D 65**, 074032 (2002).

[48] H. G. Dosch, M. Jamin and B. Stech, Z. Phys. C **42**, 167 (1989).

[49] M. Ablikim et al. [BESIII], Phys. Rev. D 104, L091104 (2021); Phys. Rev. D 107, 072005 (2023).

[50] M. Ablikim et al. [BESIII], J. High Energy Phys. 05, 022 (2024); Phys. Rev. D 109, 034029 (2024).

[51] M. Ablikim et al. [BESIII], Phys. Rev. Lett. 124, 032002 (2020); J. High Energy Phys. 11, 228 (2023).